Special issue article

SURFACE and INTERFACE ANALYSIS

Received: 26 March 2017 Revised: 19 April 2017 Accepted: 20 April 2017 Published online in Wiley Online Library

(wileyonlinelibrary.com) DOI 10.1002/sia.6243

A spectroscopic study of leak failures in cross-linked polyethylene tubing used in domestic water supply systems

Mary Jane Walzak,[a] N. Stewart McIntyre[b]* and O. Manuel Uy[c]

Recent leak failures in cross-linked polyethylene tubing from several US locations have been studied using microscopy and microscopic spectroscopy. Such failures compromise the use of a material that has been regarded as more environmentally sustainable. The failures appear to be the result of local chemical attack by aqueous chlorine that reacts with the polymer, leading to its oxidation, decrystallization and expansion of its volume. This creates stress fields that lead to chemically induced cracking of the polymer and, eventually, failure of the tubing. Each failure studied in this work was found to be associated with a micro-protrusion in the inside diameter of the tubes; it is proposed that turbulence in the water flow behind the protrusion may accelerate local mechanical and chemical attack of the polyethylene tubing. A simple inspection method is suggested to detect the presence of such protrusions before installation of the tubing. Copyright © 2017 John Wiley & Sons, Ltd.

Keywords: polymer oxidation; chloride attack; scanning electron microscopy; FTIR spectroscopy; XPS

Introduction

Cross-linked polyethylene (PEX) tubing has become the plumbing tubing of choice to deliver water within homes constructed within the past 20 years in North America.[1] Cross-linked PEX is a High Density PEX that has been highly cross-linked to improve its tensile strength and chemical resistance but rendering it more brittle. The cross-linking process is carried out either by an electron beam treatment after extrusion of the tube or one of a number of chemical reactions usually during extrusion of the polymer.[2]

Polyethylene tubing has many advantages for domestic water transport inside buildings. The material and installation costs are one-tenth that for a water service using copper pipes. Also, energy losses for PEX tubing in heated water are lower than for copper,[3] and it has a lower carbon footprint. Failures of PEX tubing have been recognized over the past two decades; the most prominent of which involved the connection to brass fittings.[1] However, PEX tubing has also been found to fail at locations remote from any connection; these have often been ascribed to the attack of oxidants such hypochlorite or chlorine dioxide[4] that are added to the water for sterilization. Some studies have quantified the effects of these oxidants on the mechanical properties,[5–7] and based on these, it has been estimated that PEX tubing, with added antioxidants, avoidance of UV exposure, and restricted concentrations of hypochlorite, could have an in-service lifetime approaching 50 years.[7]

Nonetheless, reports of 'pinhole' leaks in PEX tubing in domestic water systems have continued, according to blogs on the internet and reports of legal action.[8,9] The resulting damage to property has been particularly devastating because the volumes of water flowing through an average PEX leak appear to be much greater than for a typical leak from a copper pipe: The PEX pipe failures are often brittle catastrophic fractures, in contrast to a small orifice caused by the long term pitting process in the corrosion of copper.[8] Thus, the strong environmental and cost advantages of PEX pipe for domestic water systems are being compromised by concerns that the installation would risk costly damage to the home.

The microscopic structures and chemical properties of PEX piping leaks have been studied previously for failures that occurred in domestic water systems as well samples from accelerated testing.[10] The leaks were found to occur via cracks that propagated from the oxidized inside diameter (ID) to produce a 'brittle slit' in the outer diameter through which water flowed.

Recently, a concentration of such failures has been investigated in the Southern United States and a more invasive scientific search was launched to determine if these leaks could be associated with structural anomalies in the tubing itself. Tubing samples from seven of these locations (individual dwellings) have been collected, and a detailed study of several leaks from three of the locations was carried out.

This investigation has brought to bear on this problem, a combination of relatively new spectroscopic techniques, along with a sample preparation approach that provides a relatively clear view of the physical cross section through which the cracking process occurred. The use of some of these techniques would not have been a practical choice a decade ago. Scanning electron microscopy of insulating polymer surfaces has been made possible by the use of low-pressure environments in the sample

* Correspondence to: N. Stewart McIntyre, Surface Science Western, Faculty of Science, Western University, London, ON N6A 0J3, Canada.
E-mail: smcintyr@uwo.ca

a Surface Science Western, Faculty of Science, Western University, London, ON, N6A 0J3, Canada

b Department of Chemistry, Faculty of Science, Western University, London, ON, N6A 5B7, Canada

c Applied Physics Laboratory, Johns Hopkins University, Laurel, MD, 20123, USA

chamber.[10,11] Photo electron[12] and infrared[13,14] studies of microscopic regions have made substantial improvements in their optics in the past 5 years, allowing much better spatial resolution. Such improvements have allowed the pathway of a crack in the PEX to be traced, along with the degree of crystallinity, oxidation, and chlorine content in the face of the crack.

Our studies have found a possible correlation between the location of a crack and the presence of a micro-protrusion of the polymer phase above the average ID of the tube. It is proposed that such protrusions could cause flow anomalies leading to local concentrations of oxidants that result in a loss of crystallinity and eventual crack propagation.

Experimental

Failed PEX tubing samples were received from seven residential locations in the Southern United States. Of these samples, three locations were chosen for further study. Table 1 specifies the origin of the failures, their physical description, and the analyses undertaken on each. All PEX tubing studied had an outside diameter of 1.9 cm and an ID of 1.5 cm. The PEX in location 1 was produced by the peroxide or 'Engel' method, while the PEX from locations 2 and 3 was produced by the electron irradiation method. All tubing had been in service for at least 3 years. Sample failures were presented for analysis both in a plan view of the inside tube diameter and as cross sections prepared by cutting the tube at each end of a crack and allowing the crack to fall open, revealing the crack surface.

Optical microscopy was used to perform an initial examination of the crack and the crack face. These optical images were then used to guide microscopic studies using infrared and X-ray photoelectron spectroscopy (XPS). Scanning electron microscopy was found to cause damage to the PEX composition and, therefore, was only used after the more chemically sensitive techniques were employed. Fourier transform infrared (FTIR) absorption spectra of preselected 80 micron diameter areas were taken using the micro-attenuated total reflection objective on the Hyperion 2000 FTIR microscope attached to a Bruker Tensor II system. FTIR spectroscopy measures the vibrational frequencies of the polymer bonds; as such, it is possible to identify a region where the polymer has become oxidized or where it has changed its structure. From such spectra, measurements of the C—O and C—H bending/rocking frequencies were used to infer changes in oxidation [carbonyl index (CI)[13]] and crystallinity.[14] The depth of penetration of the micro-attenuated total reflection analysis is approximately 2 microns. XPS identifies the chemical elements present within the outermost 5 nm of the surface. As such, those elements present in a fracture zone can be identified unambiguously, if the fracture site can be opened to the spectrometer. Further, the chemical state(s) of those elements can be determined according to the exact energies of the photoelectron lines.[12] A Kratos AXIS Ultra spectrometer was used to measure the chemical composition of a chosen 300 × 100 micron area. In addition, some information on the chemical state(s) of the carbon and chlorine present could be determined. The XPS photoelectron peak intensities could be corrected to provide reasonably quantitative assays of the surface. Scanning electron microscopy was performed with a Hitachi SU3500 Variable Pressure SEM combined with an Oxford AZtec X-Max50 SDD X-ray analyzer using low-pressure mode (~100 Pa) to alleviate any charging issues from the polymer. SEM images were taken using an ultra-variable pressure detector. An accelerating voltage of 15 kV was used, which probes the sample surface to a depth of several microns. Local elemental analysis was carried out with the Oxford energy dispersive X-ray (EDX) detector using software to correct for matrix effects.

Results

Microscopic imaging

Optical microscopy studies of all PEX pipe failures showed that they were through-wall cracks (not pinholes). On the ID of the pipe, other partial through-wall cracks could be identified, thus showing that the cracking clearly originated on the water side of the tubing. The through-wall and partial cracks observed from the ID side of each sample from all locations were very similar in appearance. The crack (L1–2) shown in Fig. 1a from location 1 extends along the tube length for several millimeters with its widest gap near the median point. Magnification of that region (Fig. 1b) reveals a raised feature or protrusion (arrow) that is more clearly seen in cross section in Fig. 1c. The tube surface to the immediate right of the protrusion appears to be slightly dished. Similar protuberances were found near the median point of all leak failures from all three locations investigated.

Detailed microscopic images of two other leak failures are shown on Fig. 2 using scanning electron microscopy in low-pressure mode. These are from L1–1 and L2–2.The cross sections of the tube walls are shown with the ID uppermost in the image. Detailed examination of the crack face for the L1–1 failure (Fig. 2a) reveals lines radiating from the dished area; these are thought to be micro

Table 1. Identification of failures investigated in the study

Geographic location of sample	Failure number	Description of failure	Analysis undertaken
Location 1 (L1)	Failure 1 (L1–1)	Through-wall crack	Scanning electron microscopy-EDX
Location 1 (L1)	Failure 2 (L1–2)	Through-wall crack	Optical microscopy
			X-ray photoelectron spectroscopy
			Microscopic infrared spectroscopy
Location 2 (L2)	Failure 1 (L2–1)	Partial crack on ID	Optical microscopy
Location 2 (L2)	Failure 2 (L2–2)	Through-wall crack	Optical microscopy
			Microscopic infrared spectroscopy
			Scanning electron microscopy-EDX
Location 3 (L3)	Failure 1 (L3–1)	Through-wall crack	Scanning electron microscopy
			Microscopic infrared spectroscopy

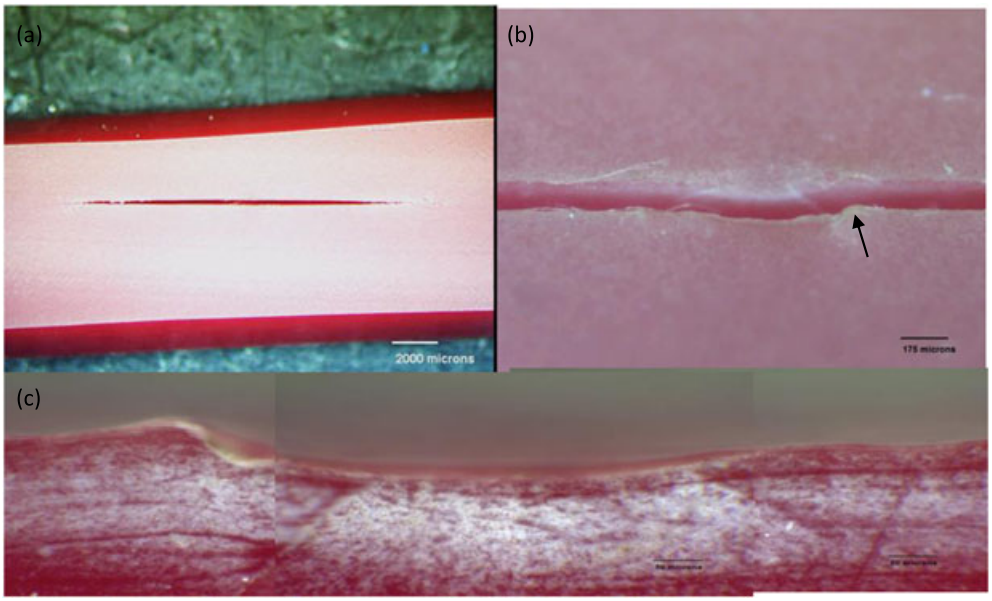

Figure 1. (a) Optical image of a through-wall crack on the inside diameter side of L1–2; (b) optical image of the region near the median point of the crack in (a); and (c) composite optical micrograph of the cross section after separation of the crack. The outermost layer of the stressed polymer in (c) appears to have a different reflectivity than the underlying polymer. [Colour figure can be viewed at wileyonlinelibrary.com]

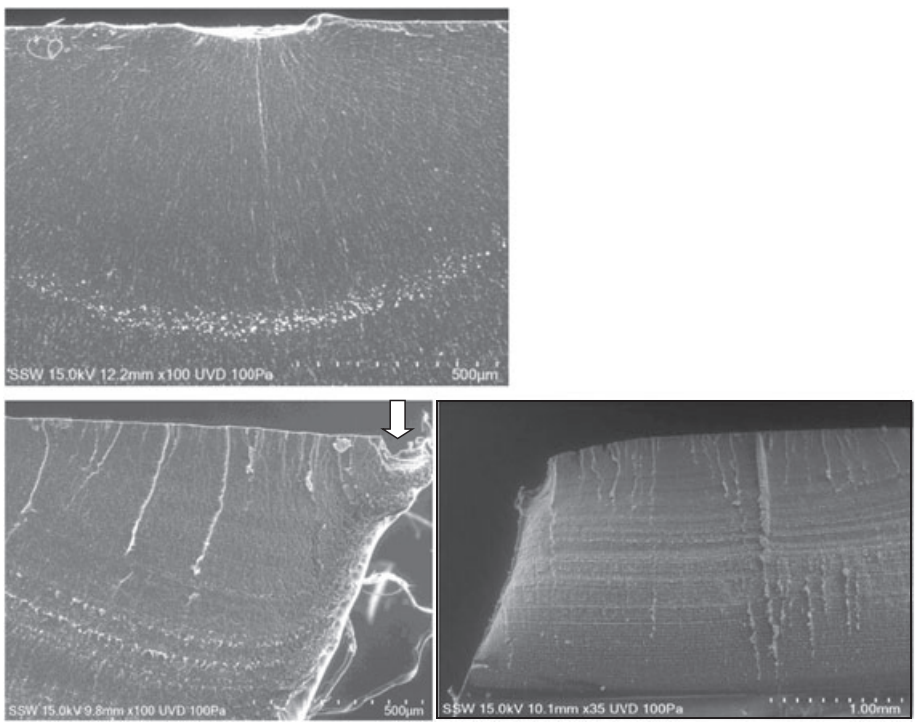

Figure 2. (a) Scanning electron micrograph of the cross section of the crack surface of L1–1 taken in low-pressure mode. The inside diameter is at the top of the image, and the protrusion is indicated by the arrow. (b and c) Scanning electron micrographs of the cross section of failure L2–2. The section split into two pieces during sectioning: each image shows one of the pieces.

cracks resulting from strain gradients that would radiate in all directions as a result of volume changes. In addition to the apparent strain features, there is a concentric arrangement of many features that are focused on the protrusion. These concentric features have been shown by EDX to be deposition products from the water (e.g. alkaline elements); these are believed to be deposited from solution near the crack tip as it advances, thus leaving a 'map' of the path of the crack. Because the crack advances are driven by a stress vector, the concentricity of the rings also suggests that the stress originates at or near the protrusion in each case. Just as with the previous crack failure examples, a dished region in the ID (arrows) is observed adjacent to the protrusion. Fig. 2b shows a similar region

found for L2–2; in this case, the depression is quite pronounced. The raised protuberance is just visible on the extreme right hand of the image. Lower magnification images of both failures (not shown here) allow the region of slow crack growth during aqueous attack to be distinguished from the region of rapid mechanical failure.

Figure 3 shows the detail of failure L3–1. As in the other cases studied, a protrusion above the ID surface was also found near the mid-point of the crack. In this case however, the protrusion was irregular in shape and appeared to have undergone localized degradation.

Spectroscopic measurements

Figure 4 shows an optical microscope image of L1–2, with the tube ID at the top of the image and the outer diameter at the bottom of the image. As with all other cracks studied, a protrusion and a dished region can be identified on the ID side near the center focus of the concentric rings on the crack surface. Quantitative compositional information of the surface of the crack face was obtained using microscopic XPS measurements. Four different areas analyzed by XPS are indicated by the numbers and the boxes. Each XPS spectrum showed peaks for carbon and oxygen, along with those for a number of minor elements that either were deposition products or were present in the original polymer as impurities. The percent oxidation of the PEX itself could be determined by subtracting the inorganic oxygen from the total oxygen. The concentrations of polymeric oxygen in the four areas were determined to be (i) 4.2 ± 0.4%, (ii) 3.5 ± 0.3%, (iii) 2.8 ± 0.3%, and (iv) 1.8 ± 0.2%. An analysis of the line shapes of the carbon C(1s) peaks showed the polymeric oxygen to be primarily singly bonded as if inserted in the hydrocarbon chain(–C–O–C–). Lower concentrations of carbonyl and carboxyl groups were also detected. Chloride was detected all along the crack face with the highest contributions in area 1(0.6% of all elements present). Analysis of the chlorine line shape showed that most of it was present as an ionic residue, but there was also some chlorine bonded to the PEX polymer.[15] Such a chlorine functionality could be an intermediate that leads to an insertion reaction with water.

Microscopic FTIR measurements were obtained on cross sections of several failures. Figure 5 shows an optical image of the cross section of failure L1–2 and indicates by numbers where a series of local microscopic infrared measurements were made. The CI [ratio

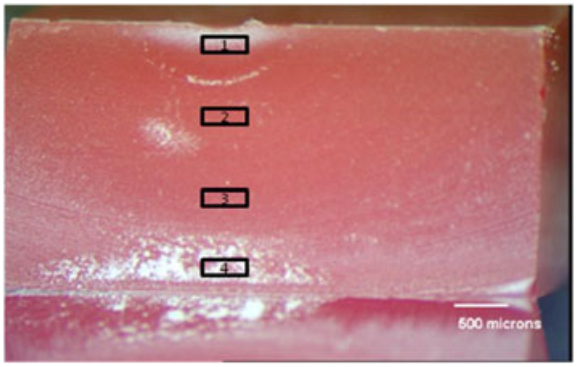

Figure 4. Optical micrograph of the same crack face as in Fig. 2a (L1–2) with the tube inside diameter at the top of the figure. Four regions are indicated that were analyzed by XPS. Region 4 lies within that portion of the crack that was believed to have opened by mechanical failure. The white areas are deposits of inorganic salts from the water passing through the leak created by the crack. [Colour figure can be viewed at wileyonlinelibrary.com]

of the carbonyl (C═O) stretching frequency to the carbon–hydrogen stretching frequency] provides an alternative measurement to XPS to measure the extent of polymer oxidation. At points nearest the ID (areas 1–4), the CI is found to be somewhat lower than points deeper into the PEX tube. This result seems to be contrary to the expectation of higher oxidation at the ID; however, none of the CI values were seen to change significantly.

Microscopic FTIR has also been used to measure the ratio of the 731 cm^{-1} peak to the 718 cm^{-1} peak in the methylene 'rocking' region. This ratio (crystallinity ratio) has been used previously to assess the local crystallinity of the PEX[13,14] expressed through the degree of cross-linking. The crystallinity ratio of the PEX at the ID (areas 1–4) is found to be lower than that in the tube interior, consistent with the expectation of more degradation of the polymer in contact with the water flow. Also, areas 1, 3, and 4 nearest the protrusion and dished region appear to be more degraded than a point on the ID further away from the protrusion.

The crack faces from failure L2–2 (shown earlier in Fig. 2b and c) were analyzed by microscopic FTIR and by SEM–EDX. Figure 6 shows the CI values measured at different points on one of the faces. The CI values are highest at the point nearest the protrusion and dished region. The CI values at this point are about three times higher than those for failure 2 location 2, i.e. polymer oxidation is

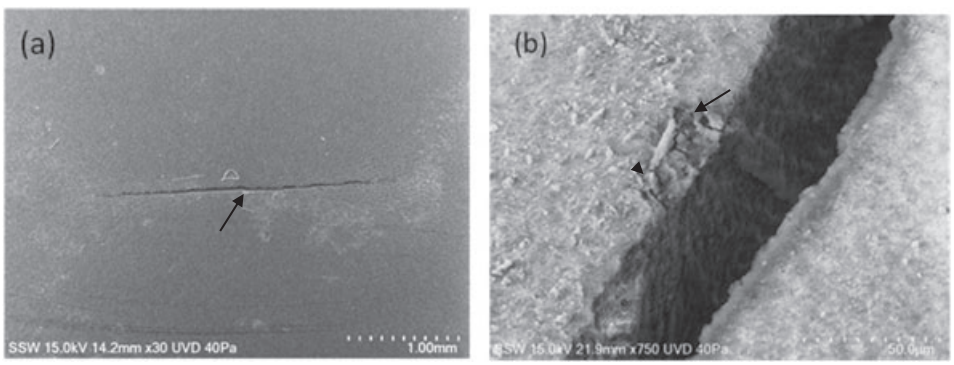

Figure 3. Scanning electron microscopic images of a crack from L3–1. (a) Image of the inside diameter crack with an irregularity near the mid-point of the crack. Both ends of the crack have crazing extending from the crack. (b) A higher magnification image of the irregularity near the crack mid-point. Unlike the smooth protrusions from the crack inside diameter surfaces found for L1 and L2, this protrusion is quite irregular.

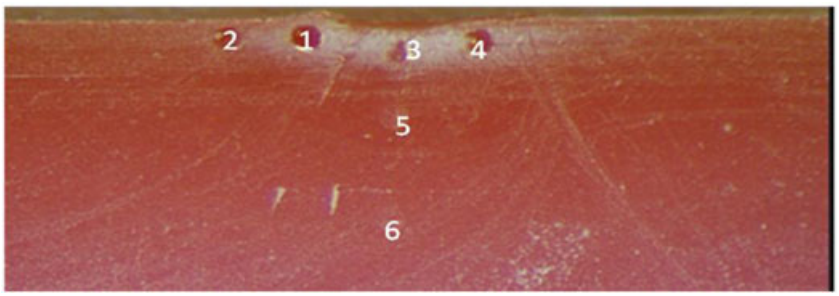

Figure 5. Optical micrograph of the crack face of failure L1–2. The tube inside diameter is at the top of the image, and the image covers the outermost 10% of the tube diameter. About 80% of tube diameter was cracked by the action of chemical attack and the remainder by mechanical forces. The numbers indicate positions where microscopic Fourier transform infrared spectra were obtained. Carbonyl indices for positions (1–6) are 0.19, 0.19, 0.19, 0.20, 0.24, and 0.24. The crystallinity ratio for positions (1–6) are 0.50, 0.56, 0.52, 0.52, 0.66, and 0.65. [Colour figure can be viewed at wileyonlinelibrary.com]

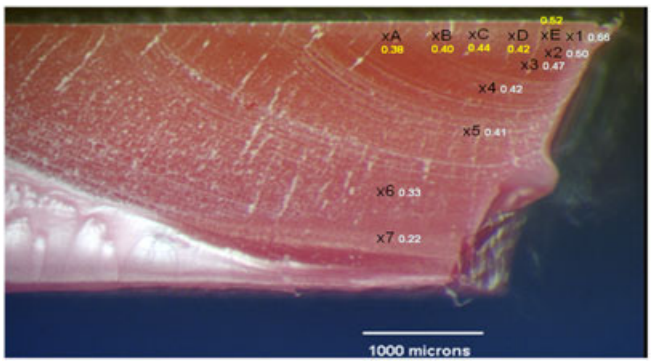

Figure 6. Carbonyl index measurements along the crack face of failure L2–2.The highest carbonyl index values are found near the protrusion, and they decrease along the inside diameter from that point (yellow numbers) and also with depth into the crack (white numbers). [Colour figure can be viewed at wileyonlinelibrary.com]

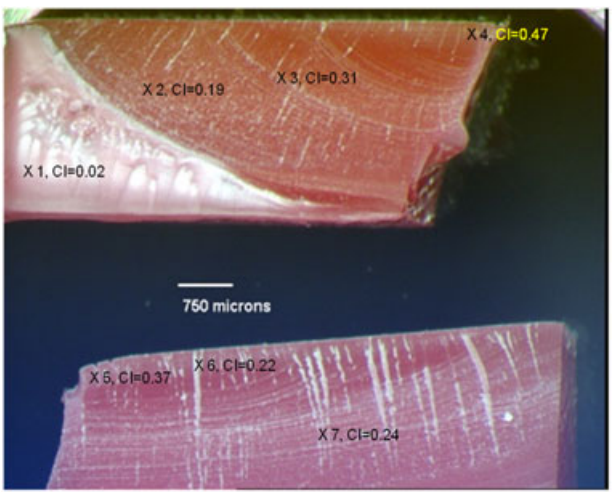

Figure 7. Chlorine concentrations along the crack face of failure L2–2 as determined by SEM–energy dispersive X-ray. The chlorine concentration is highest at the protrusion and dished area and lowest in that part of the crack that was opened by mechanical failure. These SEM–energy dispersive X-ray measurements were made after those using FTIR to reduce the possibility of degradation due to the e beam. [Colour figure can be viewed at wileyonlinelibrary.com]

much higher. In Fig. 7, the chlorine concentrations determined by EDX are shown for locations on both sides of the cross section that split near the protrusion. The highest chlorine concentration (~0.7% of all elements) is found close to the protrusion and dished region. Thus, there is a correlation between chlorine concentration and oxidation with both at a maximum near the protrusion.

Figure 8. Back -lit macrograph of a tube interior from L1. Many micro protrusions of differing size are visible. [Colour figure can be viewed at wileyonlinelibrary.com]

Discussion

The most important outcome of this work is that the initiation of cracking can be linked circumstantially to the presence of polymeric protuberances that appear on the tube inner diameter. From the microscopic images, the protrusions appear to be composed of the same material as the base polymer and an integral part of it. Such protrusions, extending tens of microns into the flowing water could act to create turbulence in the flowing water phase that could cause physical erosion and perhaps entrain micro particles and chemical oxidants, such as chlorides. The effects of even 'sand grain' surface roughness are known to affect the onset of turbulent flow in a pipe.[16] Local turbulence could produce the dished regions where attack on the polymer would be concentrated. Local oxidation would lead to decrystallization of the polymer structure through breakage of cross-linkages, followed by expansion of the volume and the creation of lateral micro stresses in the polymer and production of a crack. At some point, the chemically induced strains in the crack could induce a mechanical failure that creates the leak.

Every crack failure from the three locations studied in this work was found to have a polymeric protrusion of some size. Further, a less detailed study of failed samples from six of the seven locations showed that six of the locations had protrusions on their ID's that could be readily detected by back-lit optical inspection (See figure 8). By contrast, tubing samples recently purchased locally from stock were free of any such protuberances. This examination of tube ID's can be readily conducted on short samples using a camera on any modern mobile phone. Of course, a more elaborate inspection routine during manufacture could be conceived using a miniaturized camera on a flexible rod.

This work indicates a basis for further study of a debilitating phenomenon that has impacted the use of a material that has significantly reduced energy losses during the distribution of clean water. To this point, there has been no alternate generic explanation for the occurrence of these failures.

Acknowledgements

M. Biesinger and B. Kobe of SSW are thanked for their XPS and SEM studies, respectively.

References

[1] C. Calkins," PEX plumbing failures", https://failures.wikispaces.com/PEX+Plumbing+Failures
[2] C. Meola, G.M. Carlomagno and G. Georleo, "Cross-linked polyethylene", In Encyclopedia of Chemical Processing DOI:10.1081, Taylor and Francis, **2006**, pp. 577-5883
[3] "PEX products - history", Plastic Pipe and Fittings Association, **2011**. http://www.ppfahome.org/pex/historypex.html.
[4] J. P. Dear, M. S. Mason, *Proc. Inst. Mech. Eng.*, **2006**, *220*, 97 Many other references are provided by Reference 5.
[5] A. J. Whelton, A. M. Dietrich, *Polym. Degrad. Stab.*, **2009**, *94*, 1163.
[6] D. Castagnetti, G. Scirè Mammano, E. Dragoni, *Polym. Test.*, **2011**, *30*, 277.
[7] P. Vibien, J. Couch, K. Oliphant, W. Zhou, B. Zhang, A. Chudnovsky, *Book Inst. Mater.*, **2011**, *759*, 863–872.
[8] R.A. Clark, "Use of PEX for potable water plumbing", Submission to the California Building Standards Commission, **2005**, http://www.documents.dgs.ca.gov/bsc/pex/exhibit_e_clark_pex.pdf
[9] P. Ribbs, PHR Consultants, "The current state of PEX piping in California-section 1", **2008**, http://www.sbaypipe.org/assets/pdf/pex_report_08.pdf.
[10] S. Chung, K. Oliphant, P. Vibien and J. Zhang, "An examination of the relative impact of common potable water disinfectants (chlorine, chloramines and chlorine dioxide) on plastic piping system components", Plastic Pipes XIII, 2006, 5, **2006**.
[11] A. M. Donald, *Nat. Mater.*, **2003**, *2*, 511.
[12] F. Reniers, C. Tewell, *J. Electron Spectrosc. Relat. Phenom.*, **2006**, *125*, 1.
[13] I. W. Levin, R. Bhargava, *Annu. Rev. Phys. Chem.*, **2005**, *56*, 429.
E. Chiellini, A. Corti, S. D. Antone, R. Baciu, *Polym. Degrad. Stab.*, **2006**, *91*, 739.
[14] R. Hagemann, R. G. Snyder, A. J. Peacock, L. Mandelkern, *Macromolecules*, **1989**, *22*, 3600.
[15] M. Biesinger, "X ray photoelectron spectroscopy reference pages", http://www.xpsfitting.com/2012/04/chlorine.html
[16] S. G. Kandlikar, D. Schmitt, A. L. Carrano, J. B. Taylor, *Phys. Fluids*, **2005**, *17*, 100606.